ELSEVIER

Water Research 38 (2004) 1026–1036

WATER RESEARCH

www.elsevier.com/locate/watres

Effects of reverse osmosis isolation on reactivity of naturally occurring dissolved organic matter in physicochemical processes

James E. Kilduff[a,*], Supatpong Mattaraj[b], Andrew Wigton[a], Mehmet Kitis[c], Tanju Karanfil[d]

[a] Department of Civil and Environmental Engineering, Rensselaer Polytechnic Institute, 110, 8th Street, Troy, NY 12180, USA
[b] Faculty of Engineering, Chemical Engineering, Ubon Ratchathani University, Ubon Ratchathani 34190, Thailand
[c] Department of Environmental Engineering, Suleyman Demirel University, Cunur Campus, Isparta 32200, Turkey
[d] Department of Environmental Engineering and Science, Clemson University, 342 Computer Court, Anderson, SC 29625, USA

Received 17 January 2003; received in revised form 13 October 2003; accepted 28 October 2003

Abstract

A field reverse osmosis system was used to isolate dissolved organic matter (DOM) from two lacustrine and two riverine surface water sources. The rejection of DOM was on the order of 99% and did not vary significantly with pressure. A simple mass balance model using a single measured value of rejection predicted the concentration within the closed-loop isolation system. The effect of operating pressure and solution flux on mass recovery of DOM was evaluated in laboratory and field trials. Under controlled laboratory conditions, >99% of a lacustrine DOM could be accounted for. A fraction of the isolated DOM was not recoverable using hydrodynamic cleaning; however, this fraction was recovered by using a pH 10 NaOH wash solution. The mass recovered in the NaOH solution increased from <1% to >6% with increasing transmembrane pressures from 414 kPa (60 psi) to1000 kPa (145 psi), respectively. This is consistent with fouling that results from an increase in solution flux, and a decrease in tangential crossflow velocity. Under field conditions, mass balances were generally >95% and mass recovery was >90% in all cases. The effects of temperature on solution flux were consistent with changes in fluid viscosity; effects of temperature on membrane diffusivity or morphological properties were small. RO isolation under low pressure conditions designed to maximize DOM recovery had little effect on DOM reactivity evaluated in terms of nanofiltration membrane fouling, XAD-8 resin adsorption, activated carbon adsorption, competition with trichloroethylene for adsorption sites on activated carbon, and molecular weight distribution measured using size exclusion chromatography.

Keywords: Reverse osmosis; Natural organic matter; Isolation; Organic carbon; Fouling; Nanofiltration; Preloading; Size exclusion chromatography

1. Introduction

Naturally occurring dissolved organic matter (DOM) is widely distributed throughout all aquatic environments [1]. DOM components consist of a heterogeneous mixture of complex organic materials, including humic substances, low molecular weight (hydrophilic) acids, proteins, carbohydrates, carboxylic acids, amino acids, and hydrocarbons. Humic substances are the predominant compounds of DOM in surface waters, typically comprising 30–80% of dissolved organic carbon (DOC) [1].

DOM plays important roles in various water treatment operations, for example it can (i) compete with low

*Corresponding author. Tel.: +1-518-276-2042; fax: +1-518-276-3055.
E-mail address: kilduff@rpi.edu (J.E. Kilduff).

0043-1354/$ - see front matter
doi:10.1016/j.watres.2003.10.049

molecular weight organic pollutants for adsorption sites on activated carbon [2,3]; (ii) contribute to membrane fouling [4–6]; and (iii) produce disinfection by-products (DBPs) upon reaction with oxidants during potable water disinfection [7,8].

When studying the role of DOM in environmental processes, one approach is to use source waters directly. Another approach involves isolating DOM from source waters, which offers several advantages including reduced storage requirements and the ability to provide sufficient mass to conduct long-term studies and to allow subsequent fractionation, e.g., using XAD resins [9] and ultrafiltration (UF) [10,11].

Reverse osmosis (RO) is a pressure-driven membrane process that has many advantages as an isolation technique. RO membranes exhibit high DOM rejection [12] and RO systems can process large volumes of source water, recover organic carbon efficiently and in large quantities over relatively short periods of time, and isolate DOM without the need for strong chemical reagents [13,14]. Field-scale RO systems have been used to isolate DOM from surface and ground waters with good success [12–16]. While it is expected that the RO isolation process will cause minimal alteration of the DOM, changes in composition, e.g., increases in both organic and inorganic constituent concentrations, do occur. However, few studies have addressed whether these changes affect DOM reactivity. Kitis et al. [16] have recently reported that RO isolation preserves DOM reactivity with regard to trihalomethane and haloacetic acid formation upon reaction with chlorine. The objective of this research was to design a field-scale RO system and to investigate the role of selected operational conditions to maximize DOM recovery while minimizing any changes that could affect DOM reactivity in the context of nanofiltration membrane fouling, uptake by XAD-8 resin and activated carbon, competition with trichloroethylene during activated carbon adsorption, and molecular weight distribution.

2. Materials and methods

2.1. Field-scale RO system and DOM isolation protocol

Fig. 1 schematically depicts the field RO system. Source water was pumped by a stainless steel submersible pump (Grundfos, Inc.) and then pretreated using: (1) a virgin 10-μm polypropylene pre-filter to remove larger particles; (2) a sodium-form cation exchange softener (0.01 m^3/min capacity, Osmonics, Inc.) to remove multivalent cations (mainly Ca^{2+} and Mg^{2+}, Fe^{2+}, and Mn^{2+}) and minimize precipitation (scaling) on the membrane surface; and, (3) two cartridge filters in series (5 and 0.45-μm glass fiber or virgin polypropylene, US Filter, Inc.). During isolation, DOM solution was

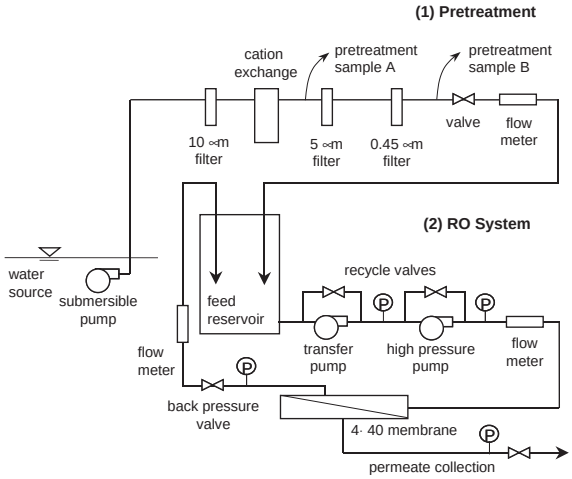

Fig. 1. Process schematic of the field RO membrane system.

recirculated through the RO system, which included a 200 L feed reservoir kept full by constant addition of pretreated source water. DOM feed solution was pumped with a high-pressure stainless-steel multi-stage centrifugal pump (Tonkaflo, Osmonics, Inc., 15 L min^{-1} at 1447 kPa). A centrifugal transfer pump provided the required inlet pressure of about 200 kPa.

The membrane module consists of a 10 cm (diameter) × 100 cm (length) (total surface area of 7.44 m^2) spiral-wound aromatic polyamide thin-layer composite membrane (Fastek™ TLC) housed in a stainless steel pressure vessel (Osmonics, Inc., Minnetonka, MN, USA). Similar membranes have proven successful in water treatment applications [17]. Clean water permeability was determined as the slope of flux versus pressure plot, linear up to 1200 kPa; $L_p = 8.86 \times 10^{-9} \pm 9.72 \times 10^{-11}$ ($m\,s^{-1}\,kPa^{-1}$). Manufacturer specified NaCl rejection is 99% (2000 ppm, 225 psi transmembrane pressure). The membrane manufacturer recommends a Q_c/Q_p ratio of 5–7 to provide adequate crossflow velocity to minimize membrane fouling; this criterion corresponds to a water recovery, $r = Q_p/Q_f$, on a *module* basis, of about 12–15%.

The maximum operating pressure that meets specified recovery criteria was quantified by combining the definition of recovery, the expression for solution flux $J_v = L_p(\Delta P - \Delta\pi)$, and an empirical (system specific) expression for feed flow as a function of pressure. Over relatively narrow ranges of pressure, the pump curve was nearly linear ($Q_f = a\Delta P + b$) and the maximum operating pressure was determined from:

$$\Delta P_{\text{allowable}} = \frac{r_{\max} b + L_p A_m \Delta\pi}{L_p A_m - r_{\max} a}. \quad (1)$$

For our system, using $r_{\max} = 0.15$, $L_p = 3.19 \times 10^{-2}$ ($L\,m^{-2}\,h^{-1}\,kPa^{-1}$), $A_m = 7.436\,m^2$, $a = -0.6461$ ($L\,h^{-1}\,kPa^{-1}$), and $b = 1226$ ($L\,h^{-1}$). Neglecting $\Delta\pi$,

the maximum allowable transmembrane pressure, $\Delta P_{allowable}$, was about 550 kPa (80 psi), corresponding to a permeate flow, Q_p, of about 2 L min^{-1}. Therefore a feed flow, Q_f, of 14.5 L min^{-1} yields a concentrate flow, $Q_c = Q_f - Q_p$, of 12.5 L min^{-1}.

An increase in permeability with increasing temperature was observed and was proportional to the change in solution viscosity, $L_{p,T2}/L_{p,T1} = \mu_{T1}/\mu_{T2}$. Therefore, as shown in Fig. 2, permeability normalized by viscosity is nearly independent of temperature. As temperature increases, the transmembrane pressure should be lowered to maintain recovery within acceptable limits. For our system, increasing the temperature from 20°C to 30°C reduced the allowable transmembrane pressure about 15%, to 466 from 550 kPa.

At regular intervals, feed and permeate were sampled for DOC, UV_{254} absorbance and conductivity analysis. In addition, feed solution temperature and pH, and permeate flow were monitored. A single isolation run was concluded by stopping the flow of pretreated source water to the feed reservoir, and then allowing the volume in the feed reservoir to decrease to approximately 20 L. After recovering the concentrated isolate, the system was flushed with about 10 L of permeate water (about 1.5 void volumes) and then cleaned by recirculating 10 L of permeate adjusted to pH 10 (using NaOH) for 20 min. After chemical cleaning, the system was again flushed with permeate water until the original permeate pH (about 6) was recovered. Overall DOM mass recovery was calculated from DOC measurements and the volumes of recovered DOM solutions (including isolated sample water, analytical samples, flush, and NaOH wash):

$$\%\ \text{Total mass recovery} = \frac{V_c C_c + \sum V_{sample}\, C_{sample} + V_{NaOH}\, C_{NaOH} + V_{flush}\, C_{flush}}{V_{source}\, C_{source}}, \quad (2)$$

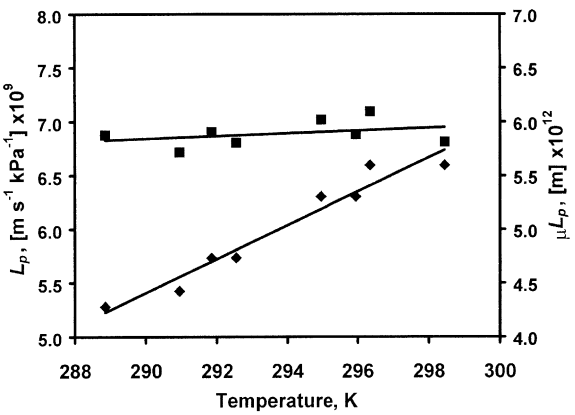

Fig. 2. Effect of temperature on water flux. Average pressure = 900 kPa (130 psi); Feedwater: pretreated Tomhannock water; recovery = 22%.

where V_c and C_c are the volume and concentration of isolate (~20 L), the sum of $V_{sample} \times C_{sample}$ is the mass organic carbon (mg) present in all samples collected during the isolation; $V_{NaOH} \times C_{NaOH}$ is the mass of organic carbon (mg) present in the NaOH cleaning solution; $V_{flush} \times C_{flush}$ is the mass of organic carbon (mg) present in the flush water; and $V_{source} \times C_{source}$ is the mass of DOM in the pretreated source water feed. Where possible, sample volumes were measured gravimetrically using an electronic balance (Ohaus, Inc.).

2.2. Water characteristics

De-ionized tap water (DI water) was prepared by filtering tap water through an activated carbon filter and two mixed-bed ion exchange columns. This water had a DOC of approximately 0.30 mg L^{-1}. Reagent grade I water was prepared by processing DI water through a Milli-Q system (Millipore, Bedford, MA) and had a DOC of approximately 0.10 mg L^{-1}. Some membrane experiments were conducted using RO permeate water.

Source waters selected for this study include the Tomhannock Reservoir, the Intercoastal Waterway, the Edisto River, and Lake Bowen, the drinking water supplies for the city of Troy, NY, Myrtle Beach, SC, Charleston, SC, and Spartanburg, SC, respectively. For isolations not carried out on-site, source waters were collected in pre-cleaned 20-L glass carboys and/or fluorinated polyethylene jerricans. All source waters and RO isolates were transported to the laboratory and were stored at 4°C in the dark without chemical addition. Selected characteristics of these source waters are tabulated in Table 1. The source waters chosen for this study have a wide range of organic carbon and specific UV_{254} absorbance ($SUVA_{254}$), with relatively low alkalinity (<100 mg $CaCO_3$ L^{-1}) and hardness (<80 mg $CaCO_3$ L^{-1}). Table 2 provides information regarding analytical methods used in this study [18].

2.3. Assessing the reactivity of DOM

In this study, the impact of RO isolation on DOM reactivity in various separation processes was characterized. Filtered (0.45-μm) source water collected at the time of RO isolation and RO isolate diluted to the same DOC and ionic strength as the filtered source water were compared side-by-side. Many of the methods involved have been described in detail in our previous publications and will only be described briefly here.

2.4. Fouling of nanofiltration membranes

DOM solution flux experiments were conducted using a cross-flow bench scale membrane test system described previously [19]. Membrane coupons were mounted in a stainless steel cell with an active filtration area of

Table 1
Raw water characteristics

Parameter	TMK[a]	IW[b]	ER[c]	LB[d]
DOC ($mg\,L^{-1}$)	2.99	20.15	3.54	2.15
$UV_{254\,nm}$ (cm^{-1})	0.074	0.935	0.165	0.039
$SUVA_{254\,nm}$ ($L\,mg^{-1}\,m^{-1}$)	2.5	4.64	4.66	1.80
Acidity (meq (g carbon)$^{-1}$)	11.2[e](28.8)[f]	8.6[e](14.3)[f]	8.2[e](24.5)[f]	ND
Alkalinity ($mg\,CaCO_3\,L^{-1}$)	35	39	23	19
Hardness ($mg\,CaCO_3\,L^{-1}$)	76	26	17	7.5
pH	7.2	7.2	7.4	7.3

Note: values reported are the averages of triplicate measurements.
[a] TMK = Tomhannock Reservoir, Troy, NY.
[b] IW = Intercoastal Waterway, Myrtle Beach, SC (as reported by Kitis et al. [16]).
[c] ER = Edisto River, Charlston, SC (as reported by Kitis et al. [16]).
[d] LB = Lake Bowen, Spartanburg, SC (as reported by Kitis et al. [16]).
[e] Titration from pH 3 to pH 7.
[f] Titration from pH 3 to pH 10.

Table 2
Analytical methods

Parameter	Standard method[a]	Equipment	Minimum reporting level
DOC[b]	5310B	TOC-5000, Shimadzu Corp., Japan Model 1010, OI Analytical, College Station, TX, USA	$0.1\,mg\,L^{-1}$
UV Absorbance[c]	5910	HP8452A, Hewlett Packard, Menlo Park, CA, USA DU 640, Beckman Inst. Inc., USA	± 0.005[d]
Total Alkalinity	2320	Laboratory glassware	2–4 mg/L as $CaCO_3$
Ca + Mg Hardness	3500 (Ca-B, Mg-B)	5100-AA, Perkin-Elmer, Germany	Ca: 0.25 mg/L as $CaCO_3$ Mg: $0.025\,mg\,L^{-1}$ as $CaCO_3$
Conductivity[e]	2510	M90, Corning Corp., USA	0.5%[f]
pH	4500-H^+	420A, Orion Corp., USA	± 0.01[g]

[a] Standard methods (APHA, 1995).
[b] Calibrated with external standards prepared using reagent-grade potassium hydrogen phthalate. Precision ranged from 0.05 to $0.15\,mg\,L^{-1}$.
[c] Measured at wavelengths of 254, 272 and 280 nm using either a 1 or 5-cm cell.
[d] Photometric accuracy (absorbance units).
[e] NaCl standards were used to correlate conductivity readings to ionic strength: IS ($mol\,L^{-1}$) = 9.5×10^{-6} ($\mu S\,cm^{-1}$).
[f] Relative accuracy.
[g] Accuracy (pH units).

$0.0155\,m^2$ (SEPA, Osmonics Inc., Minnetonka, MN). System recovery was maintained at 85%, and cross-flow velocity of $0.1\,m\,s^{-1}$ was maintained using a recycle loop, but neither retentate nor permeate was recycled back to the feed reservoir. Prior to all filtration experiments, the system was run for 5 h to allow for membrane compaction; then the transmembrane pressure, ΔP_{TM}, was adjusted to yield an initial solution flux of 45($\pm$0.7) LMH. The transmembrane pressure was then held constant throughout the run, while changes in flux were monitored.

2.5. DOM sorption by XAD-8 resin

DOM was fractionated into operationally defined humic (hydrophobic) and non-humic (hydrophilic) fractions using the methods developed by USGS researchers [9] with minor modifications. Diluted RO

isolates and 0.45 μm filtered source water were applied to a column of pre-cleaned XAD-8 resin (Supelite DAX-8, Supelco, St. Louis, MO) at pH 2. The fraction adsorbed by the resin and subsequently back-eluted from the column using a pH 11 NaOH solution is considered "hydrophobic" (HPO), while the fractions collected from the effluent of the column are considered "hydrophilic" (HPL). HPL samples were collected as a function of elution volume, representing a wide range of column distribution coefficients, k', defined as the mass of solute sorbed divided by the mass of solute in the void volume aqueous phase.

2.6. Adsorption by granular activated carbon

Adsorption isotherm experiments were conducted using the completely mixed batch reactor (CMBR) bottle-point method as described in detail elsewhere [20]. Carbon (F400 or TOG 50, Calgon Corp., Pittsburgh, PA) received from the manufacturer was sieved to a uniform particle size, sonicated to remove fines, boiled to remove soluble impurities, and then dried to constant weight. DOM solutions containing phosphate buffer to maintain pH = 7 were equilibrated 1 month under oxic conditions at room temperature (21 ± 3°C).

2.7. Competitive adsorption with trichloroethylene

Trichloroethylene (TCE) uptake by as-received and DOM-preloaded carbons was measured in headspace-free glass batch reactors employing initial concentrations ranging from 0.030 to 8 mg L^{-1}, as described previously [21,22]. For experiments using preloaded carbon, TCE was spiked in equilibrated DOM solutions, thus assuring that all competition was from pre-adsorbed organic matter. The reactors were kept well mixed for a period of 2 weeks, sufficient to reach equilibrium based on constant liquid-phase TCE concentrations. TCE was quantified by gas chromatography with electron capture detection, as described previously [21].

2.8. High pressure size-exclusion chromatography

High-pressure size exclusion chromatography (HPSEC) was employed as described previously [23,24]. Benzoic acid and poly(styrene sulfonate) were used as standards. A semi-log linear calibration curve was used to calculate the molecular weight distributions ($\log(\mathrm{MW}) = -0.312t + 7.139$; $R^2 = 0.997$) including weight- and number-averaged molecular weights, and polydispersity as described in [24].

3. Modeling DOM isolation

A mass balance relationship written for the feed reservoir under the assumption of complete mixing must account for inputs of mass from the pretreated source water ($Q_s C_s$) and the recycled concentrate (retentate) stream ($Q_c Q_c$), and output of mass in the feed stream to the membrane ($Q_f C_f$). Accumulation (loss) of mass on the membrane surface is assumed to be negligible. The mass balance is:

$$C_f \frac{dV_r}{dt} + V_r \frac{dC_f}{dt} = Q_c C_c + Q_s C_s - Q_f C_f, \tag{3}$$

where V_r is the volume of the sample reservoir (m^3). This equation can be written in terms of feed concentration by eliminating $Q_c C_c$ in favor of feed and permeate values using the overall solute mass balance $Q_f C_f = Q_p C_p + Q_c C_c$, and expressing C_p in terms of C_f using the definition of rejection, $\Re = 1 - C_p/C_f$. When the sample reservoir volume is maintained constant, the time derivative of volume goes to zero; integration of (3) with the initial condition that $C_f = C_{f,0}$ when $t = 0$ yields the feed concentration as a function of time:

$$C_f = C_{f,0}\, e^{-\beta t} + \frac{Q_s C_s}{Q_p(1-\Re)}[1 - e^{-\beta t}], \tag{4}$$

where $\beta = Q_p(1-\Re)/V_{r,0}$ and $V_{r,0}$ is the initial (and constant) reservoir volume. When the sample volume is allowed to change at a constant rate, then $V_r = V_{r,0} + (Q_s - Q_p)t$; substitution and integration of (3) with the initial condition that $C_f = C_{f,0}$when $t = 0$ yields:

$$C_f = \frac{Q_s C_s}{Q_s - \Re Q_p} + \frac{V_{r,0}^{\alpha}}{\left(V_{r,0} + (Q_s - Q_p)t\right)^{\alpha}} \times \left[C_{f,0} - \frac{Q_s C_s}{Q_s - \Re Q_p}\right], \tag{5}$$

where $\alpha = (Q_s - \Re Q_p)/(Q_s - Q_p)$.

4. Results and discussion

4.1. Pretreatment of source water

Selected water quality parameters were measured to evaluate the effect of pretreatment on the TMK DOM; these are tabulated in Table 3. The results for IW, ER and LB waters were previously reported elsewhere [16]. Removal of cations (mainly Ca^{2+} and Mg^{2+}) by the ion exchanger was >95%; however, the effect of pretreatment on other water quality parameters (including DOC and UV_{254} absorbance) was negligible. Removal of cations is expected to significantly reduce precipitation of divalent ions and destabilized natural organic matter on the membrane surface.

Table 3
Performance of pretreatment

Parameters	Source water[a]	Pretreatment sample A[b]	Pretreatment sample B[c]
$UV_{254\,nm}$ (pH 2.5)	0.090	NA	0.0779
TOC (mg L^{-1})	2.77	NA	2.70
pH	7.47	7.43	7.82
Alkalinity (mg $CaCO_3$ L^{-1})	39	39	39
Turbidity (NTU)	1.2	0.62	0.48
Temperature (°C)	17.9	18.0	20.5
Conductivity (μS cm^{-1})[d]	168	151	155
Ionic strength (M)	0.0016	0.00143	0.00147
Hardness (mg $CaCO_3$ L^{-1})	54	ND	ND
Ca^{2+} (mg $CaCO_3$ L^{-1})	39	ND	ND
Mg^{2+} (mg $CaCO_3$ L^{-1})	15	ND	ND

NA = not analyzed.
ND = below detection limit.
[a] TMK source water was filtered (0.45 μm) before analyses were conducted.
[b] Filtered with a 10 μm cartridge filter followed by cation exchange softening (see Fig. 1).
[c] Filtered with a 10 μm cartridge filter, followed by cation exchange softening as in sample A with additional microfiltration using 5 μm and then 0.45 μm cartridge filters (see Fig. 1).
[d] Normalized to 25°C.

4.2. DOM isolation

4.2.1. DOM accumulation in the feed reservoir

Fig. 3 illustrates the accumulation of DOM in the sample reservoir during an isolation run. As is typical of isolation runs in the field, during the first part of the run, the volume in the RO system was held constant by adding pretreated source water to the feed reservoir at regular intervals. During this period, the concentration of DOM in the system increased in response to the additional DOM mass in the system (at constant volume). The increase in DOM concentration was predicted using Eq. (4), using independently measured model parameters $C_{f,0}$, $V_{r,0}$, Q_s, C_s, Q_p, and $\Re$. After a period of constant volume operation, the flow of source water was stopped, and the DOM solution was concentrated to a final solution volume of about 20 L. During this period, the concentration of DOM in the system increased in response to a reduction in volume (with constant DOM mass). The increase in DOM concentration was modeled using Eq. (5), with $Q_s = 0$ and a value of $C_{f,0}$ corresponding to C_f at the end of the constant volume period of operation. As shown in Fig. 3, the model(s) capture the trends in DOC concentration quite well, using a single value for rejection, $\Re = 0.99$. In related experiments (data not shown) it was found that DOM rejection did not vary significantly over a pressure range from 414 to 1000 kPa. A sensitivity analysis revealed that the model was quite sensitive to the value of rejection; relatively small changes in $\Re$ (<10%) resulted in significant deviations from the observed behavior. The success of the model prediction suggests that losses during isolation were minimal, because the model only accounted for mass leaving the system in the permeate flow. Such modeling should be useful to identify whether additional loss mechanisms are likely to be important.

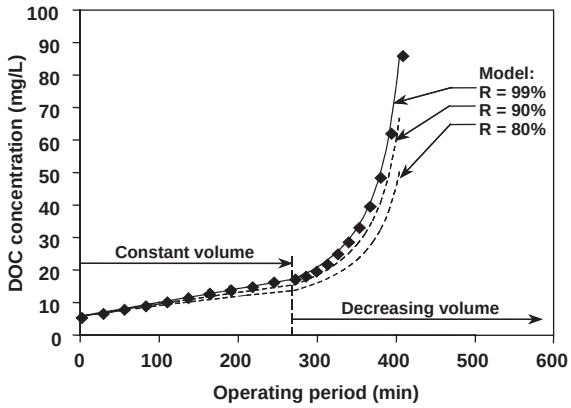

Fig. 3. Pretreated Tomhannock NOM accumulation in the feed reservoir during isolation of NOM. Symbols represent experimental data, solid line represents a model prediction based on an independently measured value of rejection (assumed to be constant); broken lines illustrate model sensitivity to the rejection parameter. Operating conditions: pressure = 414 kPa (60 psig); total volume processed = 200 L; $T = 23°C$; recovery = 8.6%.

4.2.2. DOM mass recovery

Optimizing mass recovery is important for DOM characterization, and subsequent use in reactivity studies. Laboratory continuous flow experiments were conducted to investigate the effect of pressure (and volumetric recovery) on DOM mass recovery. Temperature was maintained constant at about 20°C using a cooling coil fed with cold tap water. The total volume processed (200 L) and the mass applied to the membrane surface (600 mg) was the same in all experiments; however, as transmembrane pressure increased, the time required to conduct an experiment decreased. The DOM mass recovery was calculated using Eq. (2); results are tabulated in Table 4. The overall mass balance for these experiments was nearly 100%, demonstrating that near-complete recovery is possible using a combination of membrane flushing (hydrodynamic cleaning) followed by chemical (NaOH) cleaning of the membrane system.

Therefore, minimal DOM fractionation due to irretrievable loss of fouling components occurred. Neither NOM rejection (data not shown) nor the *total* mass recovered using this approach showed a dependence on pressure. However, the mass recovered in the concentrate solution and the subsequent clean water flush decreased with increasing pressure, while the mass recovered in the NaOH wash increased as the mass of DOM deposited on the membrane made up an increasingly greater proportion of the total mass applied (up to 6.5% at 1000 kPa). This is consistent with the greater convective transport of mass to the membrane surface and lower cross-flow velocities in the system at higher operational pressures.

Mass recovery was measured during runs conducted in the field over a range of conditions. In these experiments, the volume processed ranged from approximately 600 to 1200 L. The temperature during isolation was maintained relatively constant using a cooling coil fed with source water; however, the temperature varied depending on the source and the season. DOM from the southern waters (IW, ER and LB) was isolated at temperatures ranging from 25°C to 30°C, while DOM from the Tomhannock (TMK) water was isolated at a temperature of 15–20°C. Most runs employed a low transmembrane pressure of about 550 kPa (80 psi).

Calculated DOM mass recovery data is tabulated in Table 5. The overall mass balance achieved in field experiments is considered acceptable, but is both more variable and somewhat lower than that achieved in more controlled laboratory experiments. In part, this is because accurate gravimetric determination of process volumes was not possible in a field setting and because while hydrodynamic cleaning was done after every run, chemical cleaning was not. In addition, variability can be expected depending on operator experience and the facilities available at each field site. Propagated error in measured values (relative standard deviation, σ/μ) was $<2\%$ for mass applied, $<5\%$ for mass recovered, and $<5\%$ for overall percentage recovery. The results confirm, however, that mass recoveries $>95\%$ are

Table 4
Effect of pressure on mass recovery[a]

Sample mass, % of total applied	Transmembrane pressure				
	414 kPa (60 psi)	530 kPa (77 psi)	710 kPa (103 psi)	855 kPa (124 psi)	1000 kPa (145 psi)
Concentrate & flush	95.40	92.66	93.55	93.57	90.80
Sampling	3.60	3.38	2.68	2.23	2.22
NaOH wash	0.45	3.31	3.41	3.89	6.57
Total DOC recovered	99.45	99.36	99.64	99.69	99.59

[a] Tomhannock DOM.

Table 5
Effect of water source on NOM mass recovery

DOC (mg)	Source water							
	IW[a] Run 1	IW[a] Run 2	ER[b] Run 1	ER[b] Run 2	LB[c]	TMK[d] Run 1	TMK[d] Run 2	TMK[d] Run 3[i]
Applied[e]	8665	11,012	3346	3470	1247	2398	3329	2764
Recovered[f]	8312	10,600	3287	3259	1173	2172	3190	2695
Permeate	27.8	81.5	117.3	74.4	100.9	25.6	25.6	28.8
Recovery (%)[g]	96	96	98	94	94	91	96	98
Balance (%)[h]	96	97	102	96	102	92	97	98

[a] IW = Intercoastal Waterway, Myrtle Beach, SC (as reported by Kitis et al. [16]).
[b] ER = Edisto River, Charlston, SC (as reported by Kitis et al. [16]).
[c] LB, Spartanburg, SC (as reported by Kitis et al. [16]).
[d] TMK = Tomhannock Reservoir, Troy, NY.
[e] Mass applied from source water; error (relative standard deviation, $\sigma/\mu) = < 2\%$.
[f] Mass recovered: isolate + flush; error (relative standard deviation, $\sigma/\mu) = < 5\%$.
[g] Recovery %: 100 × Mass recovered/Mass applied; error (relative standard deviation, $\sigma/\mu) = <5\%$.
[h] Mass balance: mass recovered + mass in permeate.
[i] Mass recovered from TMK Run 3 includes a final base wash, others do not.

possible in a field setting. There does not seem to be a significant effect of water quality on DOM mass recovery for the four different waters tested, even though such properties as source water organic carbon concentration and specific UV_{254} absorbance ($SUVA_{254}$) were significantly different.

4.3. Effect of RO isolation on DOM reactivity

4.3.1. Effect of RO isolation on nanofiltration solution flux

Solution flux measured during nanofiltration using a cross-flow bench-scale test cell is shown in Fig. 4. The flux was nearly constant during filtration of clean DI water because the organic carbon content of this water was small, and because the ionic strength was low, <0.0001 M as NaCl. In contrast, solutions containing either $3\,mg\,L^{-1}$ 0.45-μm filtered TMK source water or RO concentrate diluted to $3\,mg\,L^{-1}$ showed significant solution flux decline. However, there was no significant difference between the flux decline observed for the filtered source water and the diluted RO isolate. These DOM filtration experiments provide evidence that RO isolation of the TMK water does not change the composition of the dissolved fraction of DOM in terms of the properties that govern fouling. Factors potentially affecting membrane fouling include DOM properties such as size, hydrophobicity, charge density and isoelectric point [4–6,25]. The size distribution of feed solution components relative to the pore size distribution of the membrane is important because components smaller than membrane pores can adsorb to surfaces and reduce the cross sectional area for flow, while larger components can block pore entrances and contribute to cake or gel formation.

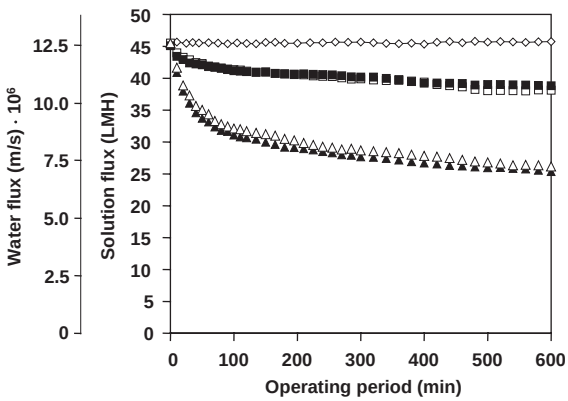

Fig. 4. Solution flux through an NF-70 nanofiltration membrane: (◇) clean water flux measured with DI water. Squares illustrate the effect of isolation; (□) pretreated Tomhannock water, 3 mg DOC/L, IS = 0.0014 M; (■) diluted Tomhannock RO isolate, 3 mg DOC/L, IS = 0.0016 M. Triangles illustrate reproducibility; (△) diluted Tomhannock RO isolate, 14 mg DOC/L, IS = 0.01 M; (▲) duplicate run using identical conditions.

Fig. 4 also shows significant flux decline during filtration of $14\,mg\,L^{-1}$ diluted RO isolate. The flux decline was greater than the $3\,mg\,L^{-1}$ runs, in part because DOM concentration and hence convective flux to the membrane surface was higher; the higher ionic strength may have also played a role. These results demonstrate that membrane filtration results using RO isolate are reproducible, and illustrate the utility of RO isolation to provide a consistent source of DOM for water treatment studies, especially when it is desirable to study concentrations greater than those of the source water itself.

4.3.2. Fractionation of DOM by XAD-8 adsorption

Fixed beds of XAD-8 resin can be employed to chromatographically separate DOM into fractions that have distinct structural and functional properties. Assuming frontal chromatography and neglecting mass transfer constraints, the elution volume, V_e, for solute breakthrough is:

$$V_e = V_0(k' + 1), \tag{6}$$

where V_0 is the column void volume and k' is the column distribution coefficient defined as the mass of solute sorbed divided by the mass of solute in the void volume aqueous phase. It has been shown that k' generally increases with decreasing solubility. If a DOM solution volume of V_e is applied to a column with a void volume of V_0, DOM components having a $k' > (V_e/V_0 - 1)$ will be retained and more hydrophilic components will elute. The hydrophilic/hydrophobic split (HPL/HPO) is defined as the ratio of mass eluted to the mass retained by the column. As shown by the data in Fig. 5, the HPL/HPO increases with k', and hence sample volume applied to the column, as more hydrophobic components break through into the effluent. The observed trend in the HPL/HPO ratio as a function of k' is similar for both the 0.45-μm filtered TMK source water and the RO isolate, suggesting that the RO isolation did not significantly affect the polarity of the source water. This finding is consistent with the observation that RO isolation of the TMK water did not change the composition of the DOM in terms of the properties that governed membrane fouling.

4.3.3. Sorption of DOM by granular activated carbon

Uptake of TMK DOM by granular activated carbon is plotted in Fig. 6. Data were plotted as a function of the non-adsorbed organic matter per unit carbon mass (C_e/D_0) because DOM is a mixture of compounds having different sorption affinities [24,26]. Sorption data were empirically fitted using a modified form of the

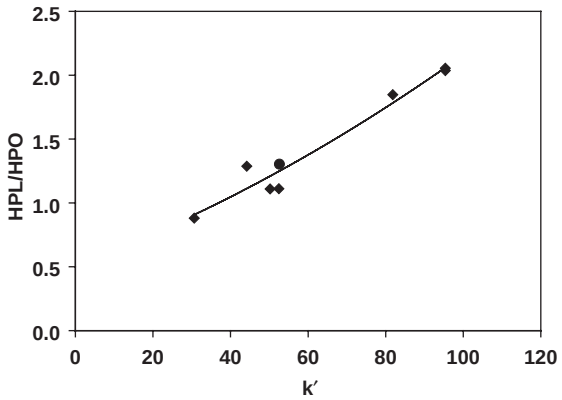

Fig. 5. XAD-8 resin chromatography of NOM. The ratio of mass eluted to mass retained, HPL/HPO, is plotted as a function of the elution volume, V_e, and bed volume, V_0, expressed in terms of the capacity factor, $k' = (V_e/V_0 - 1)$. Diamonds: RO isolate; circle: 0.45-μm filtered Tomhannock source water.

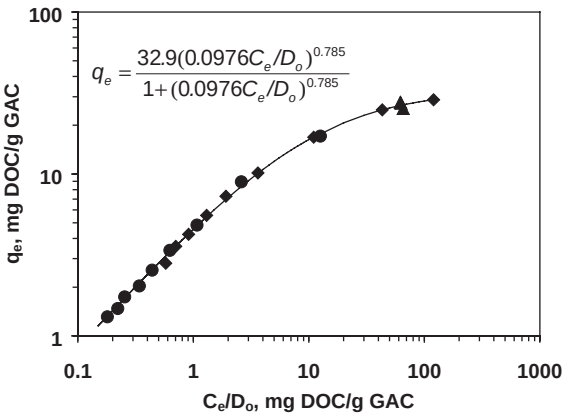

Fig. 6. Uptake of Tomhannock NOM by GAC. Conditions: circle: TMK filtered (0.45 μm) source water, $C_0 = 2.98\,\mathrm{mg\,L^{-1}}$, F400 carbon; diamond: diluted TMK RO isolate, $C_0 = 6.85\,\mathrm{mg\,L^{-1}}$, TOG 50 carbon; triangle: diluted TMK RO isolate $C_0 = 6.83\,\mathrm{mg\,L^{-1}}$, F400 carbon.

Langmuir–Freundlich isotherm:

$$q_e = \frac{Q^0(bC_e/D_0)^n}{1+(bC_e/D_0)^n}, \tag{7}$$

where q_e is the amount adsorbed at equilibrium (normalized to adsorbent mass); C_e is the equilibrium solution phase concentration; Q^0 is a capacity parameter; b is an adsorption energy parameter; and the exponential term, n, is related to the magnitude of the adsorption driving force and to the distribution of the energy sites on the adsorbent. It is clear that all the data shown in Fig. 6 are accurately described with a single set of Langmuir–Freundlich isotherm parameters.

Uptake does not appear to depend on the carbon used (F400 and TOG 50), likely because according to the manufacturer, the primary difference between the carbons is the smaller particle size of the TOG 50, which was designed for point-of-use applications. More importantly, the uptake of TMK DOM was the same whether the solution was prepared using 0.45-μm filtered source water or diluted RO isolate. Therefore, these DOM adsorption experiments provide evidence that RO isolation does not change the composition of dissolved DOM in terms of the properties that govern sorption by microporous GAC, including (1) DOM size, especially when some DOM components are too large to enter carbon micropores (on the order of 2 nm) and employ the full surface area present for adsorption; and, (2) charge density (acidity) of various DOM components, because this property affects DOM solubility and charge repulsion between DOM and like-charged functional groups on the GAC surface [20,24].

4.3.4. Impacts of preloading

The impact of DOM preloading on TCE uptake has been discussed previously in some detail [27]. Data from four preloading isotherms (three using RO isolate and one using source water) are summarized in Fig. 7. Each preloading isotherm was designed to yield a different DOM loading by varying the concentration of DOM relative to the dosage of adsorbent. As shown in Fig. 7, TCE uptake by carbon preloaded with TMK DOM was significantly reduced in comparison with uptake by as-received carbon. Greater reductions in TCE uptake were observed as the loading of DOM was increased. The reduction in uptake was greater in the low concentration

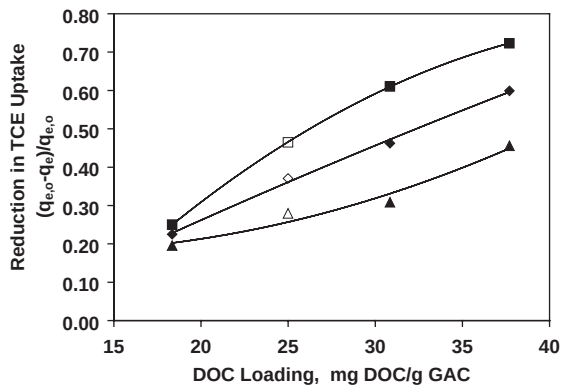

Fig. 7. The effect of NOM preloading on the uptake of TCE by GAC. TCE isotherms were measured for several NOM loadings using Tomhannock RO isolate (filled symbols) and one loading ($25\,\mathrm{mg\,g^{-1}}$) using 0.45-μm filtered source water (open symbols). The percentage reduction in TCE uptake is plotted for three equilibrium liquid phase TCE concentrations. Square: $10\,\mathrm{\mu g\,L^{-1}}$; diamond: $100\,\mathrm{\mu g\,L^{-1}}$; triangle: $1000\,\mathrm{\mu g\,L^{-1}}$. Lines are provided to highlight parametric trends.

region of the isotherm (e.g., the data shown as squares corresponding to an equilibrium TCE concentration of $10\,\mu g\,L^{-1}$), which has been interpreted as a loss of high-energy sites available to TCE, causing a significant reduction in the site-energy heterogeneity [2,21,22]. Reductions in TCE uptake by carbon preloaded with 0.45-μm filtered source water and with RO isolate followed the same trends, both with TCE concentration and DOM loading. Therefore, these preloading experiments provide convincing evidence that RO isolation does not change the composition of the DOM in terms of the species that can compete with TCE, which have been shown to be the lower molecular weight components that can access a large percentage of carbon pore volume [2].

4.3.5. Effect of RO isolation on DOM molecular weight distributions by HPSEC

Fig. 8 illustrates size exclusion chromatograms for TMK source water and RO isolate. In this figure, UV detector response was normalized to account for somewhat different concentrations used for each sample. Similar chromatograms, and hence molecular weight distributions, were found for 0.45-μm filtered source water, pretreated (filtered and softened) source water, and RO isolate. The weight-averaged molecular weights calculated using a calibration curve prepared with poly(styrene sulfonate) were 1027, 1018, and 1043 Da for TMK source water, softened TMK water, and TMK RO isolate, respectively. The corresponding number-averaged molecular weights were 581, 608, and 613. The 95% confidence interval of polydispersity ranged from 1.67 to 1.76. Statistical analysis using analysis of variance (95% confidence interval for mean) confirmed that the weight-averaged and number-averaged molecular weights were not significantly different.

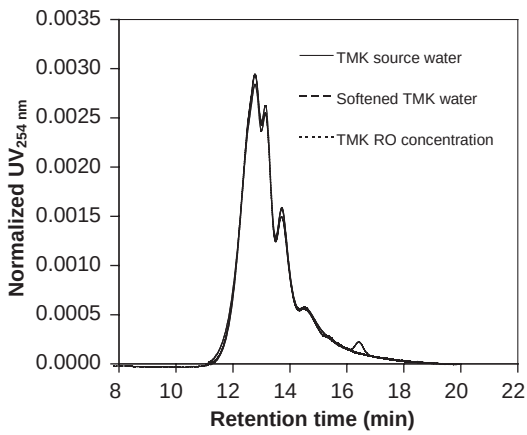

Fig. 8. Effect of TMK-RO isolation on molecular weight distributions determined using SEC calibrated with poly(styrene sulfonates).

5. Conclusions

RO isolation was employed to isolate DOM from pretreated source waters. Rejection of organic carbon was >99%, and over the range investigated, no significant effect of pressure was observed. Fouling was minimized and DOM mass recovery was high during low-pressure operation (<700 kPa or 100 psi) using a module-based recovery of about 15% or less. A simple mass balance model using a single measured value of rejection predicted the accumulation of DOM within the closed-loop system, suggesting that losses other than mass transported in the permeate flow were minor. RO isolate and 0.45-μm filtered source exhibited similar behavior in terms of (1) flux decline during nanofiltration; (2) adsorption by XAD-8 resin, as expressed in terms of the trend in the HPL/HPO ratio as a function of the column distribution coefficient, k'; (3) uptake by granular activated carbon; (4) their ability to reduce uptake of TCE by DOM-preloaded granular activated; and, (5) size distribution measured by size exclusion chromatography. These results provide evidence that RO isolation preserves DOM properties such as size, polarity, charge density and isoelectric point.

Acknowledgements

This research has been supported by the US Department of the Interior, Bureau of Reclamation, Desalination Research and Development Program (Grant 98-FC-81-0061); a Research Grant (R-828-045-01-0) from the United States Environmental Protection Agency's Science to Achieve Results (STAR) program (Office of Research and Development, National Center for Environmental Research and Quality); and the National Science Foundation, Division of Bioengineering and Environmental Systems (Grants BES-9871241 and BES-9984709). However, the manuscript has not been subjected to the peer and policy review of these agencies and therefore does not necessarily reflect their views and no official endorsement should be inferred. J.E. Kilduff and S. Mattaraj also gratefully acknowledge support from the Eastman Kodak Company. Partial support for S. Mattaraj while a graduate student research assistant at Rensselaer Polytechnic Institute was provided through a Thai Government Scholarship, Faculty of Engineering, Department of Chemical Engineering, Ubon Ratchathani University, Ubon Ratchathani, Thailand. The authors acknowledge Larry Welch, a graduate student from Department of Civil and Environmental Engineering, for his assistance in constructing the field RO system.

References

[1] Thurman EM. Organic geochemistry of natural waters. Dordrecht, Germany: Kluwer Academic Publishers; 1985.

[2] Kilduff JE, Karanfil T, Weber Jr WJ. TCE Adsorption by GAC preloaded with humic substances: effects of molecular weight. J AWWA 1998;90:76–89.

[3] Knappe DRU, Snoeyink VL, Roche P, Jose-Prados M, Bourbigot M-M. Atrazine removal by preloaded GAC. J AWWA 1999;91:97–110.

[4] Braghetta A, DiGiano FA, Ball WP. Nanofiltration of natural organic matter: pH and ionic strength effects. J Environ Eng 1997;123:628–41.

[5] Hong S, Elimelech M. Chemical and physical aspects of natural organic matter (NOM) fouling of nanofiltration membranes. J Membr Sci 1997;132:159–81.

[6] Cho J, Amy G, Pellegrino J. Membrane filtration of natural organic matter: factors and mechanisms affecting rejection and flux decline with charged ultrafiltration (UF) membrane. J Membr Sci 2000;164:89–110.

[7] Singer PC. Control of disinfection by-products in drinking water. ASCE J Environ Eng 1994;120(4):727–44.

[8] Krasner SW. Chemistry of disinfection by-product formation. In: Barrett SE, Krasner SW, Amy GL, editors. Natural organic matter and disinfection by-products. Washington, DC: ACS; 2000. p. 27–52 [Chapter 2].

[9] Thurman EM, Malcolm RL. Preparative isolation of aquatic humic substances. Environ Sci Technol 1981; 15:463–6.

[10] Buffle J, Deladoey P, Haerdi W. The use of ultrafiltration for the separation and fractionation of organic ligands in fresh waters. Anal Chim Acta 1978;101:339–57.

[11] Kilduff JE, Weber Jr. WJ . Transport and separation of organic macromolecules in ultrafiltration processes. Environ Sci Technol 1992;26:569–77.

[12] Kim J-S, Chian ESK, Saunders FM, Perdue EM, Giabbai MF. Characteristics of humic substances and their removal behavior in water treatment. In: Suffet IH, McCarthy P, editors. Aquatic humic substances: influence on fate and treatment of pollutants. Washington, DC: American Chemical Society; 1989.

[13] Serkiz SM, Perdue EM. Isolation of dissolved organic matter from the Suwannee River using reverse osmosis. Water Res 1990;24(7):911–6.

[14] Sun L, Perdue EM, McCarthy JF. Using reverse osmosis to obtain organic matter from surface and ground waters. Water Res 1995;29(6):1471–7.

[15] Clair TA, Kramer JR, Sydor M, Eaton D. Concentration of aquatic dissolved organic matter by reverse osmosis. Water Res 1991;25(9):1033–7.

[16] Kitis M, Kilduff J, Karanfil T. Isolation of dissolved organic matter (DOM) from surface waters using reverse osmosis and its impact on the subsequent formation and speciation of disinfection byproducts. Water Res 2001; 35(9):2225–34.

[17] Taylor JS, Thompson DM, Carswell JK. Applying membrane processes to groundwater sources for trihalomethane precursor control. J AWWA 1987;79(8):72–82.

[18] Eaton AD, Clesceri LS, Greenberg AE, editors. Standard methods for the examination of water and wastewater. 19th ed. Washington, DC: American Public Health Association, American Water Works Association and Water Environment Federation; 1995.

[19] Kilduff JE, Mattaraj S, Sensibaugh J, Pieracci JP, Yuan Y, Belfort G. Modeling flux decline during nanofiltraiton of NOM with poly(arylsulfone) nanofiltration membranes modified using UV-assisted graft polymerization. Environ Eng Sci 2002;19(6):477–96.

[20] Karanfil T, Kilduff JE, Kitis M, Wigton A. The role of activated carbon surface chemistry on the adsorption of organic compounds: 2. Natural organic matter. Environ Sci Technol 1999;33:3225.

[21] Carter MC, Weber Jr. WJ, Olmstead KP. Effects of background dissolved organic matter on TCE adsorption by GAC. J AWWA 1992;84:81–91.

[22] Carter MC, Kilduff JE, Weber Jr. WJ. Sorbent heterogeneity and the effects of sequential solute uptake. Environ Sci Technol 1995;29:1773–80.

[23] Chin Y-P, Aiken G, O'Loughlin E. Molecular weight, polydispersity, and spectroscopic properties of aquatic humic substances. Environ Sci Technol 1994;28:1853–8.

[24] Kilduff JE, Karanfil T, Chin YP, Weber Jr. WJ. Adsorption of natural organic polyelectrolytes on activated carbon: a size exclusion chromatography study. Environ Sci Technol 1996;30:1336–43.

[25] Jucker C, Clark MM. Adsorption of aquatic humic substances on hydrophobic ultrafiltration membranes. J Membr Sci 1994;97:37–52.

[26] Summers RS, Roberts PV. Activated carbon adsorption of humic substances, I. Heterodisperse mixtures and desorption. J Colloid Interface Sci 1988;122:367–77.

[27] Kilduff JE, Karanfil T. Trichloroethylene adsorption by activated carbon preloaded with humic substances: effects of solution chemistry. Water Res 2002;36:1685–98.